Double dynamical regime of confined water

Double dynamical regime of confined water

P Gallo and M Rovere

Dipartimento di Fisica, Università 'Roma Tre', Istituto Nazionale per la Fisica della Materia,
Unità di Ricerca Roma Tre, Via della Vasca Navale 84, 00146 Roma, Italy

E-mail: rovere@fis.uniroma3.it

Abstract
The Van Hove self-correlation function of water confined in a silica pore is
calculated from molecular dynamics trajectories upon supercooling. At long
time in the α relaxation region we found that the behaviour of the real space
time dependent correlators can be decomposed into a very slow, almost frozen,
dynamics due to the bound water close to the substrate and a faster dynamics of
the free water which resides far from the confining surface. For free water we
confirm the evidence of an approach to a cross-over mode coupling transition,
previously found in Q space. In the short time region we found that the two
dynamical regimes are superimposed and cannot be distinguished. This shows
that the interplay between the slower and the faster dynamics emerges in going
from early times to the α relaxation region, where a layer analysis of the
dynamical properties can be performed.

1. Introduction

The behaviour of water below its freezing point upon supercooling it is not easily investigated
by experimentalists since nucleation processes drive the liquid toward its crystalline phase [1].
This phenomenon prevents the observation of the transition of the supercooled liquid to the
glassy phase. Molecular dynamics (MD) simulations [2] predict a dynamical transition in
the supercooled region well described by mode coupling theory (MCT) [3]. In the idealized
version of MCT the liquid undergoes a structural arrest at a temperature T_C. This temperature
in real liquids coincides with the cross-over temperature at which the structural relaxations
of the supercooled liquid are frozen. In most liquids hopping processes start occurring close
to and below T_C and these processes ensure ergodicity of the system in this region. When
hopping is also frozen the thermodynamic glass transition takes place. Ideal predictions of
MCT are well tested on approaching T_C in the region where hopping processes are negligible.

Increasing interest in the study of water when confined arises mainly because modifications
of the behaviour of this liquid with respect to the bulk phase are closely connected to
technological and biophysical problems. In particular water seems to be more easily

supercooled when confined. This might open an experimental window in a region of the phase diagram that is experimentally not accessible for the bulk.

Both simulations and theoretical modelizations of water confined between two parallel hydrophobic walls predict new scenarios for thermodynamics and phase behaviour [4, 5]. Recent experiments on water confined between two slits of mica found that hydrophilic confinement seems to primarily suppress the hydrogen bond network associated with the freezing [6]. Similar results have been found in the case of a two-dimensional confinement in vermiculite clay [7] and in MD of water in spherical cavities [8]. A slow relaxation was found for water close to the surface of proteins [9, 10]. It has also been observed more specifically in the region around freezing that in water confined in different environments the molecules close to the substrate behave differently with respect to the molecules in the middle of the pores. The term bound water as distinct from free water has been introduced in order to distinguish the portion of water which resides in layers close to the surface, and does not show a real freezing transition, from the water far from the surface which behaves more similarly to the bulk water [11].

Recent neutron diffraction experimental studies on water confined in the hydrophilic nanopores of Vycor glass have also evidenced a severe distortion of the hydrogen bond network [12]. The slow, α, relaxation typical of glass formers has been clearly observed on water confined in Vycor upon supercooling by means of both a very refined spin-echo technique [13] and a quasi-elastic neutron scattering experiment [14]. Evidence of low frequency scattering excess typical of strong glass formers has also been observed in the same system for low hydration levels of the pore [15].

We have conducted computer simulation work on a model for water confined in Vycor [16, 17] where we found that microscopic forces due to a hydrophilic surface can induce a layering effect in water with the formation of a double-layer structure close to the surface.

In our previous works on dynamics [16, 17] we concentrated mainly on the study of the molecules which reside on average far from the solid surface identified as free water; in particular, we studied the intermediate scattering function in the α-relaxation region. MCT appears to work well in its idealized form for free water. We were able to estimate the cross-over temperatures and other MCT parameters for the full hydration [16] and for the half hydration [17] cases.

In this paper we present results obtained from MD simulation at full hydration which show clear evidence that our way of separating water molecules into two sets, namely the very slow bound water that resides in the first two layers close to the substrate and the faster free water in the inner part of the pore, is unique for our system, but only in the time window of the α-relaxation. This effect is in fact clearly visible in the Van Hove self-correlation function (VHSCF) of the confined water $G_S(r, t)$, presented here for the full hydration of the pore.

In the next section after introducing the VHSCF we show its behaviour in supercooled bulk water for a comparison with the confined case. In section 3 we give some details about our simulation of confined water and show the layering effect which takes place in our system. In section 4 we present and discuss the results obtained for the VHSCFs of the confined water. The final section is devoted to the conclusions.

2. The Van Hove self-correlation function of bulk water

The VHSCF is defined for a system of N particles or molecules as

$$G_S(r, t) = \frac{1}{N} \left\langle \sum_{i=1}^{N} \delta[\boldsymbol{r} + \boldsymbol{r}_i(0) - \boldsymbol{r}_i(t)] \right\rangle. \tag{1}$$
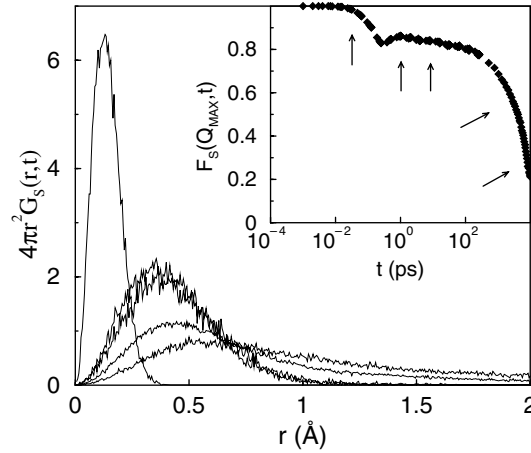
Figure 1. In the main frame the angular average of the oxygen VHSCFs calculated from MD trajectories of SPC/E bulk water is displayed for $T = 190$ K and density 1 g cm^{-3}. Curves from the left correspond to $t = 0.032, 1.024, 8.2, 2620$ and 13 107 ps. In the inset is the corresponding intermediate scattering function at the peak of the structure factor. The arrows indicate the times at which the VHSCF is evaluated. Arrows on the left correspond to curves on the left.

This function describes the correlation in the positions of the same atom at different times and more precisely $4\pi r^2 G_S(r, t) \, \mathrm{d}r$ is the probability of finding a particle at distance r after a time t if the same particle was at the origin $r = 0$ at the initial time $t = 0$. The Fourier transform of (1) is the incoherent or self-intermediate scattering function (SISF):

$$F_S(Q, t) = \left\langle \sum_{i=1}^{N} \mathrm{e}^{\mathrm{i}Q \cdot [r_i(t) - r_i(0)]} \right\rangle \tag{2}$$

which can be measured in an incoherent quasi-elastic neutron scattering experiment.

The functions (1) and (2) contain the information which concerns the single-particle dynamics and can be directly evaluated from MD trajectories. Even if they are equivalent while (2) would allow a more direct comparison with experiments, when available, the function (1) gives a more detailed and intuitive description of the motion of the particle in the fluid.

We now discuss the behaviour of VHSCF for water in its bulk supercooled phase for a comparison with the confined case. We conducted MD simulations in the NVE ensemble with 216 water molecules. The model potential used is the SPC/E. This potential, at variance with ST2 [18], shows a glassy MCT behaviour upon supercooling [2]. We cooled the system along the 0 MPa isobar characterized by a T_C estimated to be 194 K [19]. In order to equilibrate the system at such a supercooled temperature a run of 100 ns was performed with a timestep of 0.2 fs.

In figure 1 we show $4\pi r^2 G_S(r, t)$ of the oxygens as a function of r at different times. We can clearly distinguish different time regimes mastered by the caging occurring in supercooled liquids. Looking at the SISF in the inset of the same figure we see that for short times ($t < 0.04$ ps) the system is in the ballistic region; the corresponding $4\pi r^2 G_S(r, t)$ shows a sharp peak and decays rapidly to zero. For intermediate times ($0.2 < t < 100$ ps) the system is in the β relaxation region, well described by the MCT, and the 'cage effect', evidenced by the clustering of $4\pi r^2 G_S(r, t)$, is rather marked as we are right on the estimated MCT cross-over temperature. This temporal region corresponds to the plateau of the SISF. Finally, in the late
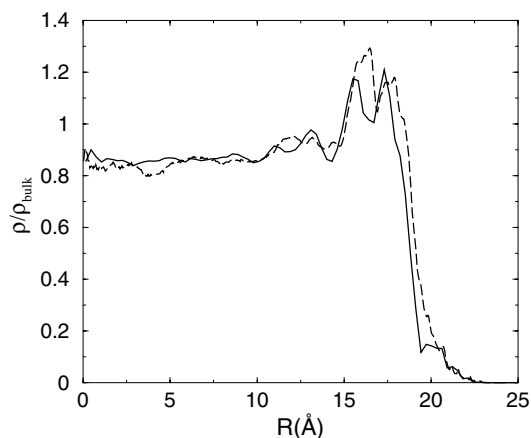
Figure 2. Density profiles for confined water normalized to the bulk value for $T = 298$ K (continuous curve) and $T = 210$ K (long dashed curve). The surface of the Vycor glass is located around 20 Å.

α-relaxation region, where the SISF is described by a stretched exponential decay, the system is entering the diffusive regime and long tails develop in the $4\pi r^2 G_S(r, t)$ which extends to longer distances at increasing time. This behaviour of the VHSCF of supercooled water is shared by most liquids approaching the MCT cross-over temperature T_C.

3. Layering effects in confined water

We describe in this section our confined system and briefly summarize the main results of the single-particle analysis conducted in the Q, t space [16, 17, 20]. We performed MD simulations of SPC/E water in a cylindrical pore of 40 Å diameter and 71.29 Å height. The pore is carved in a simulated silica glass. As described in detail in previous work [21] the surface of the pore is treated in order to reproduce the main average properties of the pores of Vycor glass. The substrate turns out to be a corrugated surface composed of silicon atoms, bridging oxygens bound to silicons and non-bridging oxygens saturated with acidic hydrogens. Different Coulomb charges are attributed to the sites of the surface representing the four types of atom; moreover, the oxygen sites interact with the oxygen sites of the water by means of a Lennard-Jones potential. We analyse in the following the full hydration case which corresponds to 2600 molecules. The pore surface turns out to be strongly hydrophilic, as can be seen from the density profile shown in figure 2. A double layer of water molecules is clearly seen close to the surface of the Vycor in the region between 15 and 20 Å, where the pore surface is located. Moving toward the centre of the pore the density reaches a value close to 11% of the bulk density at room temperature as observed in the experiments on water confined in Vycor at full hydration [12]. The figure shows that the effect of the temperature on the density profile is very small. The molecules residing in the double-layer structure display a strong distortion of the HB network [21–23].

By analysing the SISF we found that, due to the presence of strong inhomogeneities in our system, a fit of the α-relaxation region of the correlators to an analytic shape could only be carried out by excluding the subset of molecules in the double layer close to the substrate ($R > 15$ Å), identified with the so-called bound water. The subset of molecules belonging to the bound water appears to be already in a glassy state with very low mobility
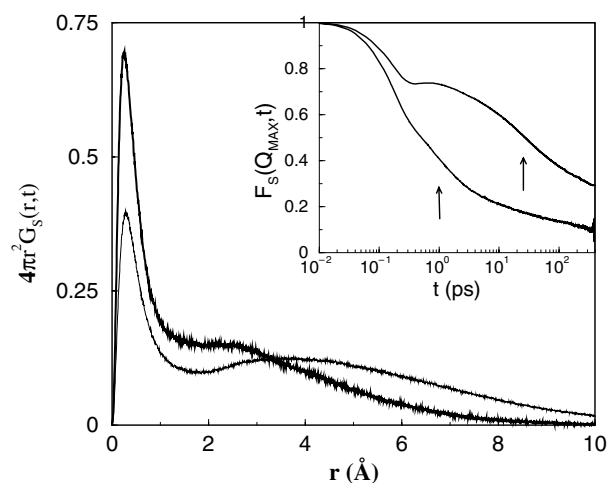
Figure 3. In the main frame is the total VHSCF for the oxygens of the water molecules for $T = 298$ K and $t = 1$ ps (lower curve) and $T = 210$ K and $t = 25.6$ ps. In the inset is the corresponding total SISF (lower T at the top). The arrows mark the times in the α-relaxation region at which the VHSCFs are evaluated.

at ambient temperature. The remaining water molecules show a dynamical behaviour typical of a glass forming liquid upon supercooling. In particular, the free water inside the pore shows a diversification of relaxation times as supercooling progresses, similar to SPC/E bulk water [2]. Focusing on the SISF we found that the intermediate time region develops the MCT predicted plateau that stretches upon supercooling. The α-relaxation region shows a stretched exponential decay. From the relaxation times extracted from the fit to this function it is possible to estimate the cross-over temperature for free water [16]. Evidence of two distinct dynamical behaviours has been found in experiments on other confined fluids [24–27].

4. The Van Hove self-correlation function of confined water

We now move to the description of the dynamics of confined water upon supercooling through the analysis of the VHSCF.

In figure 3 we show the angular average of the VHSCF as defined in equation (1), $4\pi r^2 G_S(r, t)$, of the oxygens of the water molecules confined in Vycor at $T = 298$ and 210 K. For the sake of clarity only the highest and the lowest temperatures investigated are shown in the pictures since the intermediate curves display a continuous trend. The curves have been calculated for times corresponding to the late α region as best shown in the inset where the corresponding SISFs are plotted. The more striking feature of the VHSCF is the presence in both curves of a double-peak structure. A first sharper peak, located at short distance, is followed by a second broader peak.

By considering the radial density profile of figure 2 analogously to what was done for the SISF in previous work [16, 17, 20] we also separated for the VHSCF the contribution of the molecules in the outer double layer close to the surface of the cylindrical pore between 15 and 20 Å from the contribution of the remaining molecules between the centre of the pore and 15 Å. The calculation is explicitly performed for a selected region by considering as contributing to equation (1) only water molecules that at time $t = 0$ are inside the considered region for as long as they remain in that region.
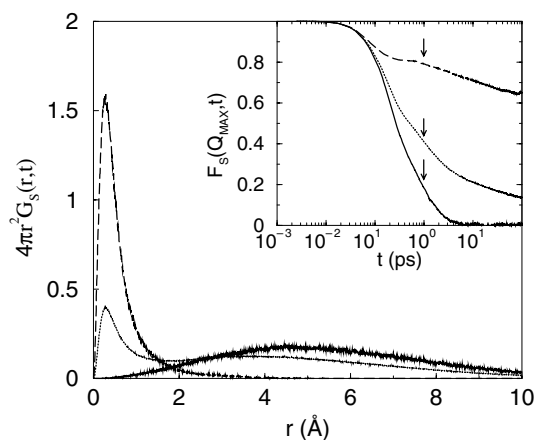
Figure 4. In the main frame is the layer analysis of the VHSCF for the oxygens of the water molecules at $T = 298$ K and $t = 1$ ps. The total correlator (dashed curve), also displayed in figure 1, is shown together with the contribution coming only from oxygens that move in the inner part of the pore (continuous curve), i.e. of the free water, and with the contribution coming from the first two layers close to the substrate (long dashed curve), i.e. of the bound water. In the inset is the corresponding layer analysis for the SISF (curves as in the main frame). The arrows mark the times at which the VHSCFs are evaluated.
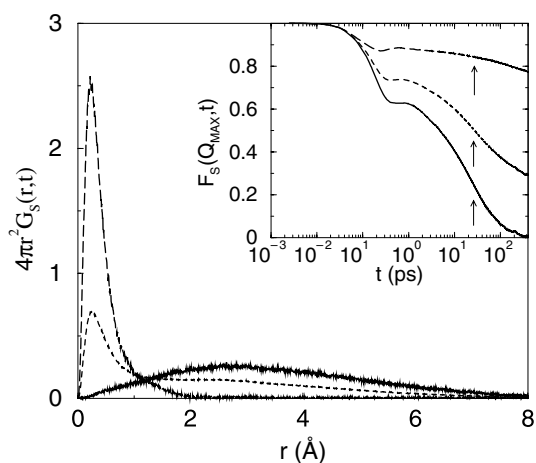

Figure 5. In the main frame is the layer analysis of the VHSCF for the oxygens of the water molecules at $T = 210$ K and $t = 25.6$ ps. In the inset is the corresponding layer analysis for the SISF. The arrows indicate the times at which the VHSCF is evaluated.

In figure 4 we report the inner layer (free water) contribution and the outer layer (bound water) contribution to the total VHSCF of figure 3 at $T = 298$ K. In the inset we show the same layer analysis performed for the intermediate scattering function (2) of the confined water. We note that the two VHSCFs are singly peaked in the α-relaxation region and that each peak corresponds to one of the two peaks of the total VHSCF. The VHSCF of the bound water is very localized and decays to zero in a few ångstrom, while in the free water the molecules are more distributed in space and the corresponding VHSCF decays slowly.

In figure 5 the same analysis is shown for $T = 210$ K. Features are similar to the previous figure. Interestingly, this division into two subsets turns out to be temperature independent in
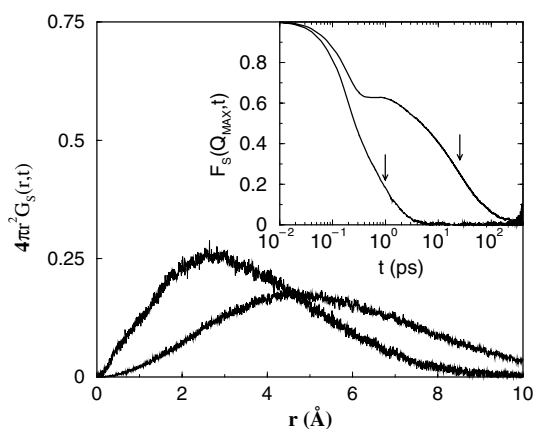
Figure 6. In the main frame is the VHSCF of free water for $T = 298$ K at $t = 1$ ps (curve on the right) and $T = 210$ K at $t = 25.6$ ps. In the inset is the corresponding SISF (lower temperature at the top). The arrows indicate the times at which the VHSCF is evaluated.

Figure 7. In the main frame is the VHSCF of bound water for $T = 298$ K at $t = 1$ ps (curve on the right) and $T = 210$ K at $t = 25.6$ ps. In the inset is the corresponding SISF (lower temperature at the top). The arrows indicate the times at which the VHSCF is evaluated.
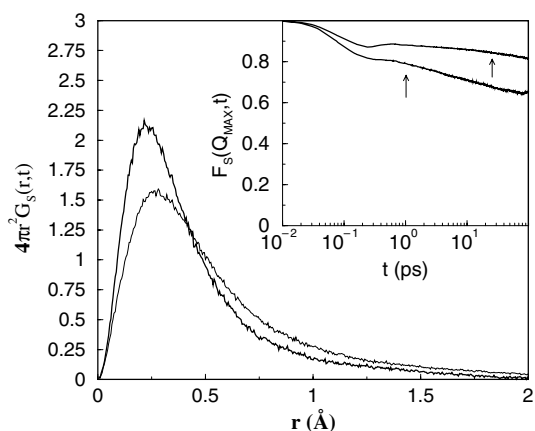
our system and therefore a general characteristic in the range of temperatures investigated for this time region.

The VHSCF at 210 K for 25.6 ps is more localized close to the origin with respect to the corresponding correlator calculated at room temperature for 1 ps, as shown in figure 6. This is due to the slowing down of the dynamics as the temperature is decreased to the region of the supercooled liquid.

The contribution due to the molecules which reside closer to the substrate (bound water) is reported separately in figure 7. It is evident that, at variance with the free water, the bound water suffers a severe slowing down of the dynamics even at room temperature. The two distributions of distances corresponding to $T = 298$ and 210 K in fact appear not to differ substantially from each other.

The comparison of the VHSCF of supercooled bound water calculated in the α region with the VHSCF of bulk water (see figure 1) shows that the molecules are much less mobile
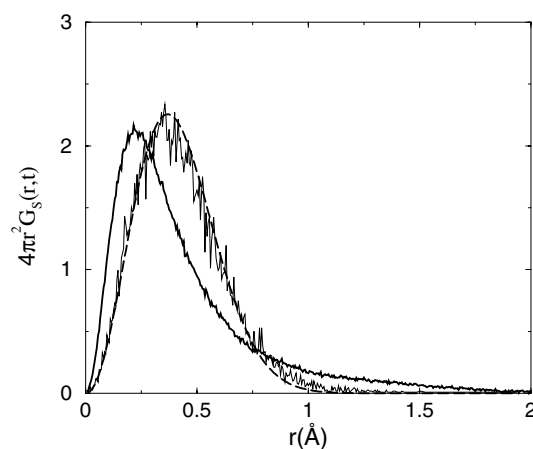
Figure 8. VHSCF of bound water for $T = 210$ K at $t = 25.6$ ps (thick curve) compared with VHSCF of bulk water for $T = 190$ K at $t = 1$ ps (thin curve). A fit to a Gaussian is superposed on the VHSCF of the bulk (long dashed thick curve).
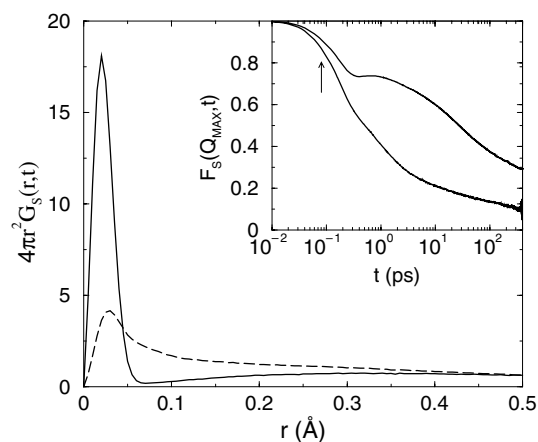

Figure 9. In the main frame is the total VHSCF for $T = 298$ K (dashed curve) and $T = 210$ K (continuous curve) both at $t = 0.08$ ps. In the inset is the corresponding SISF (lower temperature at the top). The arrow marks the time at which the VHSCFs are evaluated.

in confined bound water. This is best seen in figure 8 where we report the VHSCF of confined water at $T = 210$ K in the α-relaxation region with the most similar VHSCF of bulk water at $T = 190$ K, namely the one in the intermediate region of the rattling in the cage. We note that in spite of the fact that the curves are calculated in two different dynamical regimes they are very similar. Therefore, the confined VHSCF reproduces the features of molecules that can move essentially in the cage of the nearest neighbours. The peak of the VHSCF curve of confined bound water is shifted left, due to the higher density of bound water with respect to the bulk. It also displays a much longer tail.

In figure 9 we report the total correlator calculated for the highest and the lowest temperature investigated in the early times. At a first glance the behaviour might seem quite similar to the late α one. Nonetheless, it turned out that the shell analysis is not valid in this region. We therefore conclude that our layer analysis is limited to the temporal range of

the α-relaxation for this model while for early times the two dynamical regimes cannot be distinguished.

5. Summary and conclusions

We have presented a study of the single-particle Van Hove correlation function for a model of water confined in a silica pore of Vycor glass.

The separation into two clearly distinct subsets of water molecules in the hydrophilic pore hypothesized in a previous analysis is confirmed as unique. The VHSCF is in fact doubly peaked at all temperatures and a layer analysis of the correlators shows that water close to the substrate, bound water, only contributes to the first peak while free water only contributes to the second peak. This separation is however valid only in the slow relaxation region commonly named as α. No separation of dynamical regimes has been found in the fast relaxation region.

Due to the strong resemblance that we found in bound water with respect to water confined in biological environments [23] we infer that the double dynamical behaviour of this system is shared by water confined in biological environments like surrounding proteins.

References

  [1] For a review on metastable liquids and water in particular see
      Debenedetti P G 1997 *Metastable Liquids: Concepts and Principles* (Princeton, NJ: Princeton University Press)
  [2] Gallo P, Sciortino F, Tartaglia P and Chen S-H 1996 *Phys. Rev. Lett.* **76** 2730
      Sciortino F, Gallo P, Tartaglia P and Chen S-H 1996 *Phys. Rev.* E **54** 6331
  [3] Götze W and Sjögren L 1992 *Rep. Prog. Phys.* **55** 241
      Götze W 1991 *Liquids, Freezing and Glass Transition (Les Houches Session LI)* ed J P Hansen, D Levesque and J Zinn-Justin (Amsterdam: North-Holland)
  [4] Truskett T M, Debenedetti P G and Torquato S 2001 *J. Chem. Phys.* **114** 2401
  [5] Meyer M and Stanley H E 1999 *J. Phys. Chem.* B **103** 9728
  [6] Raviv U, Laurat P and Klein J 2001 *Nature* **413** 51
  [7] Bergman R and Swenson J 2000 *Nature* **403** 283
      Bergman R, Swenson J, Börjesson L and Jacobsson P 2000 *J. Chem. Phys.* **113** 357
      Swenson J, Bergman R and Longeville S 2001 *J. Chem. Phys.* **115** 11299
  [8] Brovchenko I, Geiger A and Paschek D 2000 *J. Chem. Phys.* **113** 5026
      Brovchenko I and Geiger A 2002 *J. Mol. Liq.* **96** 195
  [9] Settles M and Doster W 1996 *Faraday Discuss. Chem. Soc.* **103** 269
 [10] Paciaroni A, Bizzarri A R and Cannistraro S 2000 *Phys. Rev.* E **62** 3991
      Bizzarri A R and Cannistraro S 2002 *J. Phys. Chem.* B **106** 6617
 [11] Morishige K and Kawano K 1999 *J. Chem. Phys.* **110** 4867
 [12] Bruni F, Ricci M A and Soper A K 1998 *J. Chem. Phys.* **109** 1478
      Soper A K, Bruni F and Ricci M A 1998 *J. Chem. Phys.* **109** 1486
 [13] Bellissent-Funel M C, Longeville S, Zanotti J-M and Chen S-H 2000 *Phys. Rev. Lett.* **85** 3644
 [14] Zanotti J-M, Bellissent-Funel M C and Chen S-H 1999 *Phys. Rev.* E **59** 3084
 [15] Venturini F, Gallo P, Ricci M A, Bizzarri A R and Cannistraro S 2001 *J. Chem. Phys.* **114** 10010
 [16] Gallo P, Rovere M and Spohr E 2000 *Phys. Rev. Lett.* **85** 4317
 [17] Gallo P, Rovere M and Spohr E 2000 *J. Chem. Phys.* **113** 11324
 [18] Paschek D and Geiger A 1999 *J. Phys. Chem.* B **103** 4139
 [19] Starr F W, Sciortino F and Stanley H E 1999 *Phys. Rev.* E **60** 6757
 [20] Gallo P, Rovere M, Ricci M A, Hartnig C and Spohr E 2000 *Europhys. Lett.* **49** 183
 [21] Spohr E, Hartnig C, Gallo P and Rovere M 1999 *J. Mol. Liq.* **80** 165
 [22] Gallo P, Ricci M A and Rovere M 2002 *J. Chem. Phys.* **116** 342
 [23] Gallo P, Rapinesi M and Rovere M 2002 *J. Chem. Phys.* **117** 369
 [24] Mel'nichenko Yu B, Schüller J, Richert R, Ewen B and Loong C K 1995 *J. Chem. Phys.* **103** 2016
 [25] Daoukaki D, Barut G, Pelster R, Nimtz G, Kyritsis A and Pissis P 1998 *Phys. Rev.* B **58** 5336
 [26] Arndt M, Stannarius R, Groothues H, Hempel E and Kremer F 1997 *Phys. Rev. Lett.* **79** 2077
 [27] Park J-Y and McKenna G B 2000 *Phys. Rev.* B **61** 6667